OceanGliders Salinity SOP

This GitHub repository is for the OceanGliders Salinity Standard Operating Procedure (SOP).

Read the SOP here.

Community review

The community review is open from November 2021 to February 28 2022. Please read our Code of Conduct to ensure you follow the community rules.

Who is invited to review?

Constructive feedback by anyone is welcome. We encourage both experts and new gliders users who want to start observing oxygen to feedback on the document. For example: Experts are welcome to critically assess the specific methods and uncertainty ranges outlined in the SOP. New users can help to improve the SOP by providing a feedback from the user perspective. Please let us know that you use the SOP.

How to contribute

See contributer guideline here

Next steps

1. 4 months community review on GitHub starting in November 2021 until February 28 2022
2. Follow the requirements for the GOOS endorsement process as outline in Hermes 2020
3. Submission to Frontiers: Research Topic Best Practices in Ocean Observing for peer-review March 2022
4. Depositing of major SOP releases at the Ocean Best Practice System (OBPS)

The main SOP document will always reside in this GitHub repository to allow updates within the OceanGliders community at any time. After major revisions regular peer-reviewed updates are planned.

Questions?

Do you have any questions related to salinity measurements on gliders? Or do you struggle to comment the SOP document? Just raise a question here.

License

Code of Conduct

Read our Code of Conduct (CoC) [here](add link as soon as finalized). Join the discussion to finalize the CoC here

1. Authors, development process and contributions

1.1. Authors

1. Isabelle Giddy, *Southern Ocean Carbon and Climate Observatory, CSIR | Department of Oceanography, University of Cape Town, South Africa | Department of Marine Science, University of Gothenburg, Sweden*
2. Soeren Thomsen, *LOCEAN, ISPL, Sorbonne University, Paris, France*
3. Evi Bourma, *Hellenic Centre for Marine Research (HCMR)/Institute of Oceanography, Athens, Greece*
4. Louis Clement, *Marine Physics and Ocean Climate Group. National Oceanography Centre, Liverpool, UK*
5. Bastien Y. Queste, *Department of Marine Science, University of Gothenburg, Gothenburg, Sweden*
6. Nikolaos D. Zarokanellos, *SOCIB, Palma de Mallorca, Spain*
7. Anthony Bosse, *MIO, Aix-Marseille University, Marseille, France*
8. Donglai Gong, *Virginia Institute of Marine Science*
9. Gerd Krahmann, *GEOMAR Helmholtz Centre for Ocean Research Kiel, Germany*
10. Pierre Testor, *CNRS-Sorbonne Universités (UPMC Univ. Pierre et Marie Curie, Paris 06)-CNRS-IRD-MNHN, UMR 7159, Laboratoire d'Océanographie et de Climatologie (LOCEAN), Institut Pierre Simon Laplace (IPSL), Observatoire Ecce Terra, Paris, France*
11. Clark Richards, *Fisheries and Oceans Canada, Bedford Institute of Oceanography, Halifax, Canada*
12. John Kerfoot, *Rutgers, USA*
13. Travis Miles, *Rutgers, USA*
14. Daniel Haixing Wang, *Virginia Institute of Marine Science, USA*
15. Mathieu Dever, *RBR, Ottawa, Canada*
16. Joe Wang, *AMT, Advanced Marine Technology Group Limited*

1.2. SOP development process

1. Initial SOP structure was drafted by Donglai Gong and Soeren Thomsen during OceanGliders Best Practice Workshop between May 11 and 25 2021
2. Isabelle Giddy and Soeren Thomsen restructured the draft version in early July 2021 and invited more experts to join.
3. Virtual expert meeting on July 22 organized by Isabelle Giddy and Soeren Thomsen to kick start the SOP writing. Agenda
   Meeting participants: Soeren Thomsen, Isabelle Giddy, Pierre Testor, Nikolaos Zarokanellos, Daniel Wang, Louis Clement, Clark Richards, Donglai Gong, Travis Miles
4. New authors joined: Anthony Bosse, Evi Bourma, Mathieu Dever, Gerd Krahmann, Joe Wang in September / October 2021.
5. SOP moved to this repository by: Isabelle Giddy and Soeren Thomsen in November 2021. Evi Bourma and Louis Clement supported the preparation of the community review.

1.3. Contributions

Isabelle Giddy Restructured and revised the initial draft document after Soeren Thomsen and Donglai Gong. Edited the whole document and implemented comments and suggestions. Wrote the CT sensors, integration with Seaglider and SLOCUM, added comments regarding CT-pump failure, draft of DMQC and thermal lag sections. Co-chaired the OceanGliders salinity SOP expert kick-off meeting on July 22 2021. Moved the SOP to GitHub and will maintain it there until the first release and final publication.

Soeren Thomsen Scoped the initial draft together with Donglai Gong. Reviewed the overall document and comments. Coordinates the overall SOP production process. Co-chaired the OceanGliders salinity SOP expert kick-off meeting on July 22 2021. Moved the SOP to GitHub and will maintain it there until the first release and final publication.

Evi Bourma wrote the preventative measure for biofouling on GPCTD section. Provided images for the Seabird GPCTD on SeaExplorer integration and glider recovery from a small boat sections. Reviewed the whole document and gave comments.

Louis Clement wrote parts of the biofouling section related to the flight model. Reviewed the whole document and gave comments. Joined the OceanGliders salinity SOP expert kick-off meeting on July 22 2021.

Bastien Y. Queste Wrote the RBR*legato*^{3} and Sea Explorer section. Reviewed the thermal lag section and commented on the overall document.

Nikolaos D. Zarokanellos wrote parts on the pump malfunction and biofouling. Joined the OceanGliders salinity SOP expert kick-off meeting on July 22 2021.

Anthony Bosse reviewed the document and added details on the salinity comparison with external CTDs and example of pumped CTD malfunction.

Donglai Gong initiated the development of the SOP during OceanGliders Best Practice Workshop in May 2021. He joined the OceanGliders salinity SOP expert kick-off meeting on July 22 2021.

Gerd Krahmann reviewed biofouling and thermal lag sections.

Pierre Testor wrote the proposals for funding the OceanGliders best practice coordination activities. Joined the OceanGliders salinity SOP expert kick-off meeting on July 22 2021. Reviewed the whole documemt.

Clark Richards provided images for the RBR*legato*^{3} on SeaExplorer integration. Joined the OceanGliders salinity SOP expert kick-off meeting on July 22 2021.

John Kerfoot wrote parts of the DMQC section. Joined the OceanGliders salinity SOP expert kick-off meeting on July 22 2021.

Travis Miles wrote parts of the thermal lag correction section. Joined the OceanGliders salinity SOP expert kick-off meeting on July 22 2021.

Daniel Haixing Wang wrote parts of the thermal lag correction section. Joined the OceanGliders salinity SOP expert kick-off meeting on July 22 2021.

Mattieu Dever wrote the RBR*legato*^{3} section.

Joe Wang provided a brief overview of the integration of CT-sensors with the Petrel Glider including an image.

2. Introduction

This OceanGliders standard operating procedure (SOP) document for salinity aims to guide the user through the current community practices in use for measuring and deriving good quality salinity measurements using gliders. For the derivation of salinity, simultaneous measurements of conductivity, temperature and pressure are required, which are commonly acquired by conductivity-temperature-depth (CTD) sensors. The relative location of the conductivity, thermistor and pressure sensors, offsets in the time-responses of the sensors and the thermal-inertia effect impacts the derived variable, the correction for which is described in Section 8.

The first section describes the available sensors and their integration with gliders. The following sections outline general pre deployment / real time / post deployment and data dissemination protocol recommendations. Finally, the future outlook for salinity measurements by gliders is discussed.

Table 1: List of the known sensor/glider combinations we aim to cover in this document.

Sensor / Glider	Slocum	Autosub/ ALR (NOC)	Seaglider	Deepglider	SeaExplorer	Spray	ATM Petrel	Information
Seabird - Glider Payload CTD and Slocum Glider CTD (pumped)	X Slocum specific		X	X	X	X		Link
Seabird - CT-Sail (unpumped)			X		X			CT-Sail (provided by Sea-Bird on request)
RBR*legato*[3] (unpumped)	X		X		X		X	Link

3. Sensors and integrations

3.1. CTD Sensors

On gliders, currently three types of CTD-sensors are in use (see Table 1). CT sensors can be unpumped (Sections 3.1.1.1; 3.1.2) or pumped (Section 3.1.1.2). Unpumped CT sensors have lower power consumption requirements as well as reduced susceptibility to blockages/failures because of the larger throughflow pipe (Section 6.2.4). There is also reduced background vibration and noise, which is advantageous when measuring microstructure [Fer *et al.*, 2014]. However, the disadvantage of the unpumped sensors is in the post processing correction for the effects of thermal-inertia because the flow rate through the inlet is not known and has to be estimated from the glider's flight model (Section 8.1). Pumped CT sensors on the other hand, have a constant through-flow rate, allowing for a simpler correction of thermal-inertia. Nevertheless, both pumped and unpumped sensors require corrections for thermal-inertia (Section 8.1).

3.1.1. Sea-Bird

Conductivity, temperature and depth (CTD) sensors distributed by Sea-Bird electronics is currently the most widely used sensor on gliders.

3.1.1.1. Unpumped

The CT-Sail, a free-flushed (unpumped) CTD (SBE41), was the first science payload installed in the Seaglider [Janzen and Creed, 2011] and remains widely in use. The separate temperature and conductivity sensors are installed on the upper side of the glider pressure hull and integrated with the internal glider data acquisition and flight control system. On the CT-Sail the temperature sensor is positioned beneath and parallel to the conductivity sensor. The conductivity sensor itself is positioned within a metal housing with hole cut-outs to allow for flushing. The pressure sensor is located ~40 cm in front of the thermistor, requiring a slight spatial alignment with the sensors. Power consumption is 21 mW while profiling.

Sea-Bird provided CTD SBE41-sensor accuracy ratings: Conductivity: ± 0.0003 S m^{-1} over a range of 0 to 7 S m^{-1}; Temperature: ± 0.002°C over a range of -5 - 45°C and Pressure: ± 2 dbar over a range of 0-2000 m.

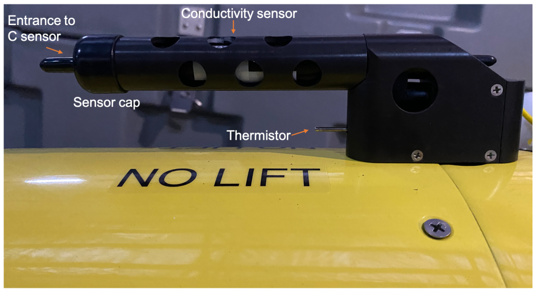

Fig. 3.1 CT-Sail with metal housing, thermistor located beneath the salinity sensor. (Figure credit: Isabelle Giddy)

3.1.1.2. Pumped

The Glider Payload CTD (GPCTD) is a modular, self-contained CTD with memory and an integrated pump. The GPCTD improves on the CT-Sail through simpler installation requirements as well as a pump which allows for constant flow through the conductivity sensor. The CT sensors are ducted and pumped on the GPCTD with the intake positioned to minimize measurement errors caused by the vehicle's thermally contaminated boundary flow [Janzen and Creed, 2011]. Power consumption is 175 mW when continuously recording at 1 Hz.

Sea-Bird provided GPCTD accuracy ratings are: Conductivity: ± 0.0003 S m^{-1} over a range of 0 to 9 S m^{-1}; Temperature: ± 0.002°C over a range of -5 - 42°C and Pressure: ± 0.1% of full scale range, up to 2000 m.

Fig. 3.2 Slocum Glider CTD (pumped). The thermistor is located within the inflow valve on the left (Image credit: Isabelle Giddy)

A variation of the GPCTD, the Slocum Glider CTD has been developed for installation on SLOCUM gliders. The sensor is installed on the side of the SLOCUM. The continuously pumped CTD consumes 240 mW sampling continuously at 0.5 Hz.

3.1.2. RBR*legato*^{3}

The RBR*legato*^{3} is an integrated CTD and logger package designed specifically for gliders with a hydrodynamic profile. It is available in slow (1 s) and fast (0.1 s) response temperature options as well as normal (2 Hz) and fast (16 Hz) sampling speeds. The RBR*legato*^{3}, unlike the previously mentioned sensors, has an inductive cell rather than conductive, with significant implications for sensor calibration of salinity. Its advantages are a large unpumped flow cell, reducing occurrence of spikes due to bubbles and fouling. As such, it is very good for near-surface applications and slow glider speeds, as well as for glider missions involving instrumentation sensitive to vibration (e.g., shear probes) or noise (e.g., acoustic packages). The RBR*legato*^{3} has low power consumption (45 mW) when sampling at 2 Hz. Its profile and low power have many benefits, but the inductive cell and relative youth of the sensor leave some open questions regarding long term accuracy. As a logger, the RBR*legato*^{3} can also integrate other RBR sensors (such as the oxygen optode RBR*coda*3^3 T.ODO) enabling fast 16 Hz sampling even if the glider platform does not have the capability onboard and reduces the number of sensor ports required to connect to the glider.

The RBR*legato*^{3} has a manufacturer-provided accuracy of ± 0.002°C (ITS-90) over a range of -5 to +35°C.

3.2. Sensor integrations with gliders

3.2.1. Mounting location

3.2.1.1. Spray

- expert missing

3.2.1.2. Seaglider

On Seagliders the Sea-Bird electronics supplied CT-Sail is mounted on the upper side of the glider pressure hull. Flow past the CT sensors relies solely on the movement of the glider. Sea-Bird no longer lists the CT-Sail but is manufactured on request by integrators. The Glider Payload CTD replaces the CT-Sail and was developed for easier integration and improved data output associated with the addition of a pump to control flow past the sensors. The GPCTD is installed between the pressure hull and the fairing in the aft-flooded payload bay.

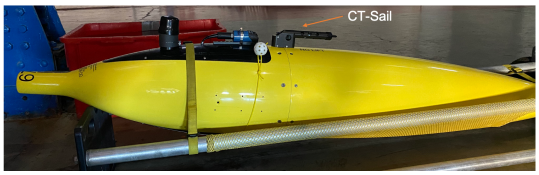

Fig. 3.3 Unpumped CT-Sail mounted above the pressure hull on a Seaglider. (Image credit: Isabelle Giddy)

3.2.1.3. Slocum

On slocum gliders, an adaptation of the GPCTD, the Slocum Glider CTD, is installed beneath a wing on the lateral side of the glider.

Fig. 3.4 Slocum Glider CTD installed on a Slocum G2 beneath the wing. (Image credit: Isabelle Giddy)

3.2.1.4. SeaExplorer

On SeaExplorer gliders, the CTDs are typically installed in the flooded nose cone area (Fig. 3.5, left), though the RBR*legato*^{3} can also be configured to be installed through one of the top/side "puck" ports to leave the nose available for other sensors (e.g. acoustic payloads) as shown in Fig. 3.5, right.

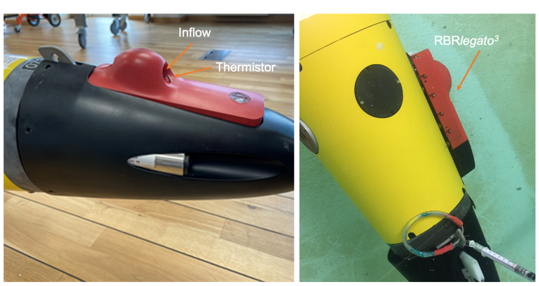

Fig. 3.5 RBR*legato*^{3} CTD on SeaExplorer (Image credits: Bastien Queste (left) and Clark Richards (right))

In the case of the Sea-Bird GPCTD, the sensors are integrated on the wet payload part located on the front nose of the SeaExplorer glider, with the integrated pump providing a constant flow through the conductivity cell.

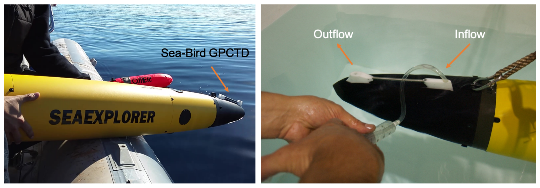

Fig. 3.6 Left: Sea-Bird GPCTD on SeaExplorer; Right: GPCTD on SeaExplorer during in lab preparation (Image credit: Evi Bourma)

3.2.1.5. Petrel Glider

The small-size RBR*legato*^{3} CTD is embedded in the front fairing of the Petrel glider. The CT sensors are exposed outside the fairing to sense the ambient seawater. This integration design can minimize the impact of the CTD on the streamline of gliders.

Fig. 3.7 RBR*legato*^{3} Petrel Glider integrated an RBR*legato*^{3} CTD in the front fairing. (Image credit: Joe Wang)

3.2.2. Sensor sampling rates

While each sensor has a range of sampling rates that can be set, the real limitation is set by the processing system associated with the platform.

Sensors integrated on Seagliders are limited to once every 5 seconds (0.2 Hz), unless the seaglider is installed with a scicon board (discontinued).

SeaExplorers have a dedicated ARM processor and can handle up to 16Hz.

Older Slocums with a persistor typically sample once every 4 seconds (0.25 Hz). This can be changed to once every 2 seconds (0.5 Hz) when the science persistor has 'free' time, meaning when you do not have too many other sensors. Recent models (eg. G3) can handle faster sampling rates.

3.2.3. Sensor storage

Sensors are stored dry with sensor caps on or tape to cover open valves, and protected from dust and freeze.

4. Pre deployment protocol

4.1. Sensor Calibration

Most users send their CT-sensors to manufacturers to get high quality/high precision calibrations. Few organizations have the ability to do in-lab conductivity and temperature calibrations, especially for the unpumped CTD found on Seagliders because of its direct integration into the glider fairing (see Section 3.1.1.1).

For the RBR*legato*[3] sensor with an inductive cell, the calibrations can only be done in the field or by using the SeaExplorer's coefficients that correct the influence of the vehicle on the sensor's inductive field. The accuracy of these coefficients is unproven. The recommended strategy is to sample deep CTD in proximity, which becomes problematic in shallow dynamic shelf sea waters. Nevertheless, correction is simple: a scaling factor is applied to conductivity.

Users should note that conductive cells (mostly unpumped, but the pumped ones as well to an extent) change conductivity calibration (again just a scaling factor) when they take a hit, because it can change the shape/volume of the conductivity cell. There is increased risk for this to occur during deployments by crane from large vessels.

4.2. Antifouling

Materials immersed in water experience a series of biological and chemical processes, resulting in the formation of complex layers with attached organisms. Biofouling that can affect salinity through 1) blocking the CT valve (see Section 6.2.4) and 2) impacting the flight model, which estimates the glider's speed assuming a steady flight in still water. This glider's speed is then used to correct the thermal-inertia effects of unpumped CT instruments (see Section 8.1). Biofouling will tend to increase the drag coefficients and decrease the lift coefficients of the flight model. A time-dependent/ incremental flight model can handle these effects. In the correction proposed by [Bennett *et al.*, 2019], the coefficients of every profile are calculated and can correct the effects of the biofouling on the flight model. In GEOMAR / Gerd Krahmann implementation, if there is a 5% increase in the drag coefficient over the deployment, then it is treated as time dependent and the optimization of the flight parameters is handled accordingly.

Pre-mission, if one expects biofouling on the glider platform (e.g. in regions of very high productivity), one can put zinc-oxide cream over the seams of the glider so that there are fewer locations with tiny turbulence where larvae have time to attach. During post mission procedures, in order to eliminate biofouling effects for the next mission and clean the GPCTD, it is suggested to be thoroughly rinsed in (with a special water dispenser) and out (with a water jet) with fresh water. Then, the antifouling solution can be inserted with a special dispenser (e.g. syringe) into the plumbing of the sensor.

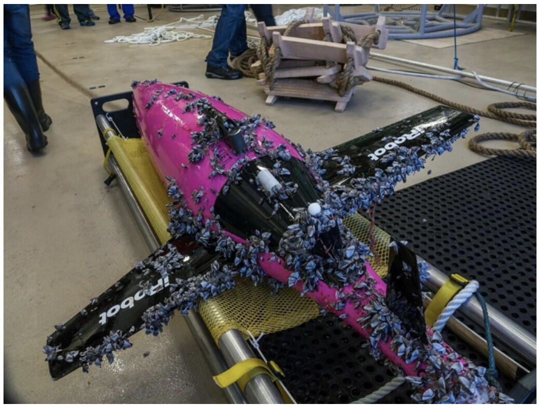

Fig. 4.1 Biofouling example from a long deployment in the Subtropical Zone in the Southern Ocean (Image credit: Sebastiaan Swart/CSIR-SOCCO).

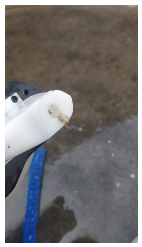

Fig. 4.2 Biofouling on the GPCTD intake after 36 days in the Aegean Sea (Image credit: Evi Bourma).

5. Missions execution

This section covers the activities of those deploying and recovering the gliders in the field in addition to best practices for glider pilots.

5.1. Deployment

The deployment procedure of gliders is platform specific and the manufacturer guidelines should be followed. Commonly, gliders are deployed from large ships or small boats. Recently, gliders have been deployed from an AutoNaut (UEA). If sensor caps are required, these should be removed before the glider enters the water.

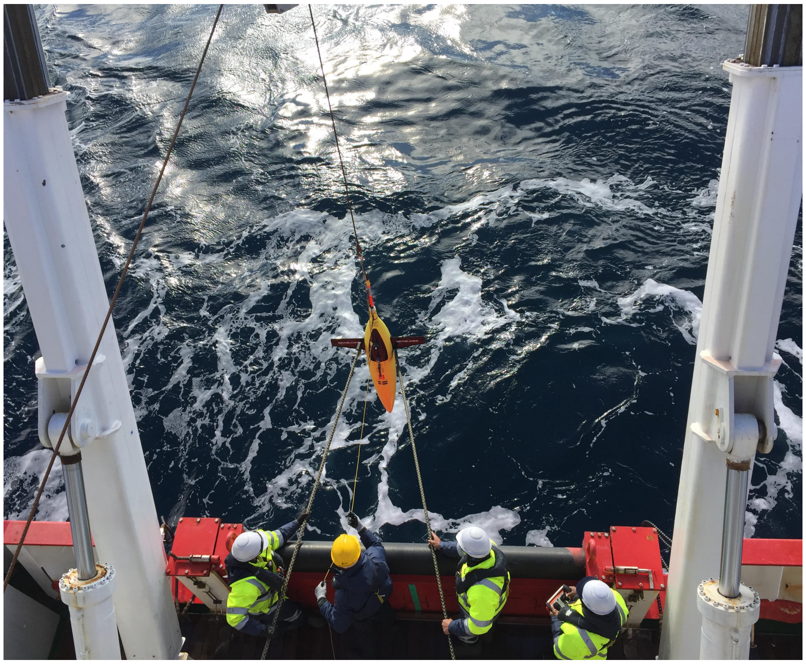

Fig. 5.1 Deployment of Seaglider using a winch (S.A Agulhas II). (Figure credit: Isabelle Giddy)

Gliders' recovery is often performed by a small boat, while the manufacturer's guidelines should be followed during the procedure.

Fig. 5.2 Recovery of the glider from a small boat. (Figure credit: Evi Bourma)

5.1.1. Colocated CTD profiles for post-mission sensor correction

On deployment and recovery of the glider, an in situ comparison-CTD cast should be completed. On a ship, the CTD rosette is often accompanied by salinometry that is used to calibrate the ship CTD (ref). If the glider is deployed from a small boat, a smaller hand deployable CTD can be used. In the case that a CTD cast cannot be completed at the same time as deployment/recovery, the characteristics of deep water masses (below the thermocline and depending on the region of deployment) can be compared with high quality reference CTD profiles (shipborne CTD, mooring data or delayed-mode Argo float data). Those reference data should preferentially sample the same regional basin and be affected by the same local circulation pattern. Ideally, offshore deep profiles sampling water mass with low variability in their properties should be used.

5.2. Piloting

In this section specific piloting requirements during the mission execution are mentioned which are needed to allow quality control.

5.2.1. Flight model calibration dives

Upon deployment it is important to perform a number of calibration dives (follow steps outlined Depth Averaged Currents (DAC) SOP to constrain the flight model) in order to be used for the correction of salinity in the field Section 4.1.

5.2.2. Data to correct for sensor drift and offset

Corresponding with Section 5.1.1, the glider should complete a dive at the beginning and end of deployment in parallel with an independent CTD cast.
Coordination between the recovery group and the pilots is essential. In the case where this is not possible, the deep water (from 600-1000 m) measurement from the nearest CTD in space (not time) can also be used as deep water masses tend to be relatively invariant at longer timescales (weeks-months). Further comparison can be made in the case of multiple gliders being deployed in parallel, these can be piloted such that they cross paths every intermittently for inter-comparison.

5.2.3. Gather data to help correct for sensor response time

Regular up- and down casts are needed to estimate and correct for the sensor response time. Combined up- and downcasts should be carried out at least every week and particularly at the beginning and at the end of the deployment. One to two days per week appear to be a reasonable compromise between energy saving and calibration quality. If bio-fouling is expected during the deployment it is better to collect up-down pairs earlier rather than later.

6. Required Metadata, Real Time Data Processing & Quality Control

This chapter has to be co-developed with the OceanGliders Data Management Task Team, the Data Assembly Centers (DACs) and RTQC Best Practice group to ensure to build on their work.

6.1. Required Metadata and Real Time Data Processing

- XXX

6.2. Real Time Quality Control (RTQC)

- XXX

6.2.1. Global range check

- XXX

6.2.2. Outlier and spike check

- XXX

6.2.3. Stuck value test

- XXX

6.2.4. Pump malfunction

While pumped conductivity cells are desirable as thermal-inertia is generally reduced, pumped conductivity cells are more prone to malfunction than unpumped cells. The two primary issues experienced by the pumped cells are 1) pump failure and 2) biofouling.

You could examine the pump failure in the following way: Doing a simple experiment in the lab by using a syringe with blue dye to evaluate the performance of the CTD pump (Fig. 6.1). In addition, the user can modify the configuration of the CTD pump's speed to examine the pump's behavior. The CTD pumps have two modes, mainly for testing purposes. The 'PumpSlow mode is generally the mode that we use for profiling as it is energy efficient.

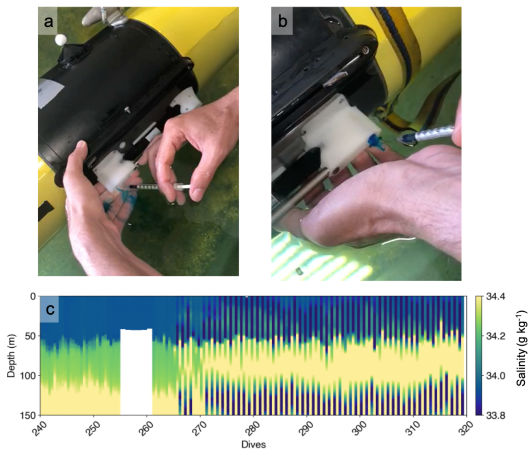

Fig. 6.1 a) A working pump CTD: There is a flow of the input dye. b) A pump CTD that failed: There is no flow of the blue dye. (Image credit: Nikolaos Zarokanellos). c) Example of uncorrectable thermal-inertia as a result of a blocked inflow (perhaps by a particle) which, after a few weeks regained flow (this data has been corrected for thermal-inertia already where possible). A pump failure may look like this too. (Isabelle Giddy)

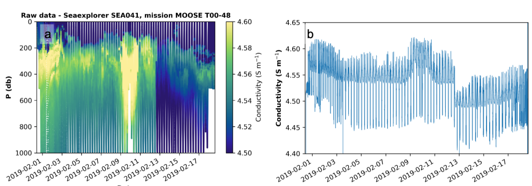

Fig. 6.2 a) Conductivity measured during a SeaExplorer mission in which the pumped CTD failed. The failure of the pumped CTD (on SeaExplorer) was possibly due to a particle in the pump system. b) Time series of conductivity shows that when the pump failed, there was a sudden drop in conductivity. It is hard to know if the slope observed afterward is natural due to the cleaning of the CTD cell, thus making correction by a constant offset questionable. A similar conductivity jump has also been observed on a Slocum glider equipped with an unpumped CT after a likely landing (abort same depth).

Regarding the biofouling of a particle, if the user observes drifting in the conductivity in the real-time data, especially on the stable deep waters, the glider pilot can try to increase the flow of the water that passes from the CTD to avoid this sensor shifting. To do that, the glider pilot needs to have a few steep dives (there is a limitation on how steep we can do). After a few dives, this procedure may result in the particles being flushed out, and then the steepness of the dive can be returned back to normal. If that does not work, the glider pilot needs to plan for a recovery.

A failed pump can sometimes be fixed by a simple reboot of the system. If particles block the inflow, because the inflow is narrow, it is not easily flushed. In most cases, thermal-inertia as a result of pump malfunction cannot be corrected for. A failed pump can be identified in realtime and the sensor switched off (refer to Fig. 6.1 above).

7. Post-recovery operations and calibrations

7.1. Integration with OceanObs

At first, user should report that their mission is over. support@oceanobs.org

7.2. Biofouling

Post recovery photos are essential for biofouling assessment Section 4.2.

7.3. Field Calibration

If you recover the glider from a small boat or a research vessel follow protocols described in Section 5.1.1.

7.4. Sensor storage

Sensors are stored dry with sensor caps on or tape to cover open valves, and protected from dust and freeze.

8. Delayed Mode Quality Control

8.1. Correction for dynamic errors

Salinity derived from temperature and conductivity is prone to dynamic errors that are a result of profiling in a dynamic environment characterised by spatial temperature and salinity gradients. While dynamic errors in conductivity and temperature are usually small relative to natural variations, they can compound into large relative errors in derived salinity. This is because, in many regions of the ocean salinity does not vary as much as conductivity and temperature. Dynamic errors can, for example, create false density instability in profiles and false variation in mixed layer depths. This is particularly important in beta oceans, where density is set by salinity variations (e.g. in polar regions; Gulf of Oman). Both pumped, unpumped, electrode-based and inductive CTDs that measure conductivity and temperature (see Section 3), are prone to dynamic errors that can be greater than the instrument calibration accuracy and therefore need to be corrected for [Johnson *et al.*, 2007], [Woo and Gourcuff, 2021].

Four main sources of error are (i) spatial offsets in sensor location on the profiling platform, (ii) timestamping of sensor measurements, (iii) the themister thermal-inertia effect and (iv) the conductivity cell thermal-inertia effect.

We suggest applying the thermal mass correction method similar to that proposed by [Garau *et al.*, 2011], which was intially developed by [Lueck and Picklo, 1990] and [Morison *et al.*, 1994], to account for the delayed temperature equilibration of the conductivity cell. (see Chapter 5 DMQC). The correction depends on the speed with which the water flows through the conductivity cell. For pumped CTDs, the flow through the CT cell is known and constant, thus corrections like [Garau *et al.*, 2011] can be simplified to use only constant thermal-inertia corrections, however these corrections are generally worse around the thermocline because: 1) the glider speed may change as a result of stratification; 2) there is a rapid vertical change in temperature and/or salinity. In the case of unpumped CTDs, for increased accuracy, we recommend using the modelled velocity of the glider through the water (based on the flight model) to estimate the flushing speed of the CT cell, which can be used to correct for the temperature offset (reference to Depth Averages Current (DAC) SOP). The flight model can be improved by following pre-deployment and piloting protocols as per the DAC SOP. The amplitude of the error, α, and the time offset constant, τ, are used to correct for thermal mass offset. These parameters can be estimated by minimizing the difference between consecutive up and down dives in temperature and salinity space, although minimizing in salinity and depth space can be preferable in some environmental conditions (with different stratification characteristics) and was also applied by [Morison *et al.*, 1994]. We use up-down dives (the top of the yo) for this correction because the measurements are closest in time and space in the upper layer/thermocline where thermal-intertia errors tend to be most important. One can elect to apply this minimization per dive or over the whole mission. Per dive tends to give cleaner data but can sometimes mask real signals (if regressed in depth, z). Applying the minimization per mission makes the assumption that the shape of the sensor doesn't change and that the model is representative and so only one set of parameters is needed to represent a whole mission. In cases in which the hydrodynamic coefficients change (e.g. if there is biofouling), per dive or multiple dive segments may be a preferable choice.

It should be noted that because such corrections require interpolating to a regular time grid, the (1) interpolation method and (2) correction scheme, can introduce energy at specific frequencies in post processing which can bias any form of spectral analysis for TS data down the line (https://oem.rbr-global.com/floats/files/5898249/34668603/1/1586804683000/0008228revA+Dynamic+corrections+for+the+RBRargo+CTD+2000dbar.pdf).

The corrections we propose are therefore:

8.1.1. Spatial alignment correction

Apply offset to account for the spatial offset in sensor location on the platform, if needed.

When the conductivity cell and thermistor are not colocated on the instrument, they measure the same water parcel but at different times. Similarly, the pressure sensor measurements for that water parcel will not occur at the same time. The time difference depends on the flow speed and distance between the sensors. If there is a variable profiling rate, the time difference will not be constant and the correction relies on the flight model. Pumped CTDs reduce the complexity of the correction by pumping water past the conductivity cell and thermistor at a known rate. The unpumped RBR*legato*[3] reduces the error associated with the sensor misalignment by moving the thermistor from the float end cap to the mast of the conductivity cell.

8.1.2. Interpolate to consistent timestamps

Interpolate to consistent timestamps between thermistor, conductivity cell and pressure sensors.

8.1.3. Correction for thermal inertia

Thermistors and conductivity cells have finite, but different, response times and are addressed separately.

8.1.3.1. Apply correction for thermistor thermal inertia

Heat must diffuse through a metal housing to reach the thermistor itself before a temperature change is registered. If a sensor has a long response time relative to the time scale for temperature changes, then the measured temperature will both lag the true signal, and have a reduced high-frequency amplitude. The error manifests itself as spikes in salinity and density especially when crossing interfaces with a sharp change in temperature with depth. The simplest correction it to shift temperature in time to ensure that the conductivity and temperature readings were taken simultaneously.

8.1.3.2. Apply correction for conductivity cell thermal inertia

Because conductivity is a function of both temperature and salinity, when the conductivity cell exchanges heat with the water it samples, errors can occur which manifest themselves as spikes in salinity or density when the instrument enters a mixed layer from stratified waters.

Initially, the effects of thermal inertia can be visualised as a scatter plot of temperature and salinity, colored by dive phase (whether the glider is performing a dive or a climb). The effectiveness of the correction can then be checked similarly. Often, the correction is not perfect: the remaining error can be reported as a RMSE of the difference between dives and climbs, as in [Giddy *et al.*, 2021].

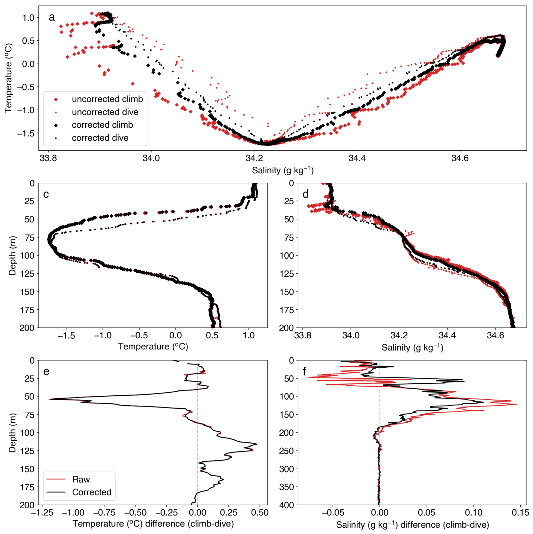

Fig. 8.1 Assessment of thermal inertia effects and its correction for one consecutive dive/climb sequence a) Uncorrected salinity and temperature; b) Corrected salinity and temperature; c) Uncorrected (red) and corrected (black) temperature-depth profile (both dive and climb); d) Uncorrected (red) and corrected (black) salinity-depth profile (both dive and climb); e) the temperature difference between a climb and a dive (uncorrected: red; corrected: black); f) the salinity difference between a climb and a dive (uncorrected: red; corrected: black). (Figure credit: Isabelle Giddy).

There are a number of implementations used by the community to correct for conductivity cell thermal inertia. These have generally been developed for specific sensor-platform integrations and are listed below as such.

8.1.3.2.1. Unpumped Seabird CT cell on seagliders

Basestation processing developed by Charlie Eriksen (unpublished). The correction is based on an iterative thermal diffusion scheme through layers in the water column.

8.1.3.2.2. Pumped Seabird CT cell mounted on Slocum gliders

GEOMAR implements the [Garau *et al.*, 2011] method with updated coefficients.

8.1.3.2.3. Pumped and unpumped Seabird CT cell

8.1.3.2.4. SOCIB

SOCIB implements the [Garau *et al.*, 2011] method.

8.1.3.2.5. UEA Glider Toolbox

UEA glider toolbox implements [Garau *et al.*, 2011], using GEOMAR / Gerd Krahmann polynomials and an empirical regression of alpha and tau absolutes and offsets.

8.1.3.2.6. Integrated Marine Observing System (IMOS)

[Woo and Gourcuff, 2021] provide recommendations for the correction of thermal-inertia to both pumped and unpumped Seabird CT cells, following alignment of temperature measurements to the conductivity cell. In the case of pumped CTDs, the flow through the cell is constant and the method of [Lueck and Picklo, 1990], generalised by [Morison *et al.*, 1994] is implemented. In the case of unpumped CTDs, the method developed by [Morison *et al.*, 1994] is recommended over the more recent method by [Garau *et al.*, 2011], which modified [Morison *et al.*, 1994] to take into account variable flow speeds as a result of an unpumped CTD. Testing by [Woo and Gourcuff, 2021] found that the improvement in the correction algorithm did not improve the results and is computationally inefficient.

8.1.3.2.7. New method by Daniel Wang, Donglai Gong and Travis Miles (to be published)

An improved methodology is proposed by Daniel Wang, Donglai Gong and Travis Miles to correct the thermal lag error in pumped glider CTDs with a specific focus on glider data from the MAB and other highly stratified oceans. The method has been tested and validated on Slocum gliders with pumped Seabird CTDs. An updated thermal lag correction algorithm was developed based on [Garau *et al.*, 2011] and it introduces a new cost function for calculating the pairwise thermal lag correction coefficients in highly stratified oceans. The algorithm also takes the vertical variability of the thermocline into account for more robust corrections in the presence of internal waves. Specifically, the parameters within the cost functions are normalized and depth is zero-referenced to the thermocline depth. Based on the observed temperature gradient at the thermocline, the algorithm then decides whether to use the normalized T-S or S-Z relation for the cost function. The improved method was able to eliminate most of the mismatches of salinity and density profiles between adjacent down up casts, and also fixed the problem of mismatching water mass identities in the T/S space. Salinity spikes up to 0.5 and density inversions up to 0.2 kg m^{-3} the vertical profiles were successfully corrected.

8.1.3.2.8. RBR*legato*^{3}

Recommended procedures by RBR themselves using internal and external temperature of the logger as detailed in their "Data processing and dynamic corrections for the RBR*legato*^{3} CTD" report. Note that this work is still on-going, so the procedures are expected to be updated in the near future.

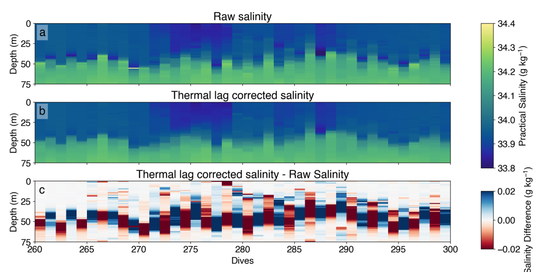

Fig. 8.2 Example of the thermal inertia effect on salinity before and after correction (Isabelle Giddy)

8.2. Sensor offset and drift correction

The sensor offset and drift are corrected using comparison CTD casts (see Section 5.1.1, Section 5.2.2). Temperature and salinity are regressed with a colocated CTD that has a known accuracy. Typically the salinity and temperature profiles are compared directly or in TS space. The sensor correction should be quoted together with details on the comparison cast. If no correction is made, this can also be reported.

8.3. 2nd quality control, inter-comparison

While thermal lag correction improves spikes and the dissymmetry between adjacent profiles, remaining outliers/spikes can be corrected for (depending on the use case) using rolling medians, depth-bins and the removal of outliers (e.g. some methods in GliderTools [Gregor *et al.*, 2019]). The application of a median filter as proposed by [Liu *et al.*, 2015] can further improve the salinity error correction in regions of strong thermoclines with temperature changes above ~2^{o}C within 3 m.
Sensor drift corrections to shipboard CTD casts and/or other gliders should be reported (see GROOM-FP7 D5.3).

9. Data sharing

OceanGliders strongly encourages all glider operators to share their data to the public and provide open access both in real time and delayed mode. The best practices of data sharing are described in the [OceanGliders data management user manual](add link to the OceanGliders data management user manual).

10. References

[BSE19]
James Bennett, Fritz Stahr, and Charlie Eriksen. Determining Seaglider Velocities Automatically. 2019. URL: http://hdl.handle.net/1773/44948.

[FPU14]
Ilker Fer, Algot K. Peterson, and Jenny E. Ullgren. Microstructure Measurements from an Underwater Glider in the Turbulent Faroe Bank Channel Overflow. *Journal of Atmospheric and Oceanic Technology*, 31(5):1128–1150, 2014. URL: https://journals.ametsoc.org/view/journals/atot/31/5/jtech-d-13-00221_1.xml, doi:10.1175/JTECH-D-13-00221.1.

[GRZ+11]
Bartolomé Garau, Simón Ruiz, Weifeng G. Zhang, Ananda Pascual, Emma Heslop, John Kerfoot, and Joaquín Tintoré. Thermal Lag Correction on Slocum CTD Glider Data. *Journal of Atmospheric and Oceanic Technology*, 28(9):1065–1071, 2011. doi:10.1175/JTECH-D-10-05030.1.

[GSdP+21]
I. Giddy, S. Swart, M. du Plessis, A. F. Thompson, and S.-A. Nicholson. Stirring of Sea-Ice Meltwater Enhances Submesoscale Fronts in the Southern Ocean. *Journal of Geophysical Research: Oceans*, 2021. doi:10.1029/2020JC016814.

[GRKN+19]
Luke Gregor, Thomas J. Ryan-Keogh, Sarah-Anne Nicholson, Marcel du Plessis, Isabelle Giddy, and Sebastiaan Swart. GliderTools: A Python Toolbox for Processing Underwater Glider Data. *Frontiers in Marine Science*, 6:738, 2019. doi:10.3389/fmars.2019.00738.

[JC11]
Carol D. Janzen and Elizabeth L. Creed. Physical oceanographic data from Seaglider trials in stratified coastal waters using a new pumped payload CTD. In *OCEANS'11 MTS/IEEE KONA*, 1–7. Waikoloa, HI, 2011. IEEE. URL: http://ieeexplore.ieee.org/document/6107290/, doi:10.23919/OCEANS.2011.6107290.

[JTL07]
Gregory C. Johnson, John M. Toole, and Nordeen G. Larson. Sensor Corrections for Sea-Bird SBE-41CP and SBE-41 CTDs. *Journal of Atmospheric and Oceanic Technology*, 24(6):1117–1130, 2007. URL: https://journals.ametsoc.org/doi/10.1175/JTECH2016.1, doi:10.1175/JTECH2016.1.

[LWL15]
Yonggang Liu, Robert H. Weisberg, and Chad Lembke. Glider Salinity Correction for Unpumped CTD Sensors across a Sharp Thermocline. In *Coastal Ocean Observing Systems*, pages 305–325. Elsevier, 2015. URL: https://linkinghub.elsevier.com/retrieve/pii/B9780128020227000171, doi:10.1016/B978-0-12-802022-7.00017-1.

[LP90]
Rolf G. Lueck and James J. Picklo. Thermal Inertia of Conductivity Cells: Observations with a Sea-Bird Cell. *Journal of Atmospheric and Oceanic Technology*, 7(5):756–768, 1990. doi:10.1175/1520-0426(1990)007<0756:TIOCCO>2.0.CO;2.

[MAL+94]
James Morison, Roger Andersen, Nordeen Larson, Eric D'Asaro, and Tim Boyd. The Correction for Thermal-Lag Effects in Sea-Bird CTD Data. *Journal of Atmospheric and Oceanic Technology*, 11(4):1151–1164, 1994. URL: http://journals.ametsoc.org/doi/10.1175/1520-0426(1994)011<1151:TCFTLE>2.0.CO;2, doi:10.1175/1520-0426(1994)011<1151:TCFTLE>2.0.CO;2.

[WG21]
L. Mun Woo and Claire Gourcuff. Delayed Mode QA/QC Best Practice Manual Version 3.0 Integrated Marine Observing System. *Australian Ocean Data Network*, 2021. URL: https://catalogue-imos.aodn.org.au:443/geonetwork/srv/api/records/b82ec5c4-3b6a-4a39-a4e7-f1adba2d5372, doi:10.26198/5C997B5FDC9BD.

11. Acknowledgement

The coordination of producing this document was supported by the European Commission via the EuroSea.eu project under H2020 funding (Grant agreement 862626) and GROOM || Horizon 2020 research and innovation programme (Grant agreement No 951842).

The contribution by I.S. Giddy was made possible through support by the Swedish Research Council (VR 2019-04400) and NRF-SANAP (SNA170522231782, SANAP200324510487).

This work also contributes to the Mediterranean Ocean Observing System for the Environment (MOOSE), which is funded by the CNRS-INSU and the French Ministry for Education and Research (ILICO Research Infrastructure).